International Journal of Nanomedicine

Dovepress
open access to scientific and medical research

Open Access Full Text Article

ORIGINAL RESEARCH

Green synthesis of multifunctional PEG-carboxylate π back-bonded gold nanoconjugates for breast cancer treatment

This article was published in the following Dove Medical Press journal:
International Journal of Nanomedicine

Mani Gajendiran[1,2]
Heejung Jo[2]
Kyobum Kim[2]
Sengottuvelan Balasubramanian[1]

[1]Department of Inorganic Chemistry, University of Madras, Guindy Campus, Chennai 600025, India; [2]Division of Bioengineering, School of Life Sciences and Bioengineering, Incheon National University, Incheon 22012, Republic of Korea

Background: Surface functionalization of gold nanoparticles (AuNPs) has emerged as a promising field of research with enormous biomedical applications. The folate (FA)-attached polymer-gold nanoconjugates play vital role in targeting the cancer cells.

Methods: AuNPs were synthesized by using di- or tri-carboxylate-polyethylene glycol (PEG) polymers, including citrate-PEG (CPEG), malate-PEG (MAP), and tartrate-PEG (TAP), as a reducing and stabilizing agent. After synthesis of polymer-AuNPs, the freely available hydroxyl and carboxylate groups of CPEG, MAP, and TAP were used to attach a cancer cell-targeting agent, FA, via a 1-Ethyl-3-(3-dimethylaminopropyl) carbodiimide/N-hydroxy succinimide coupling reaction to obtain FA-CPEG-AuNP, FA-MAP-AuNP, and FA-TAP-AuNP nanoconjugates, respectively. The 5-fluorouracil (5FU) was attached to π back-bonded carbonyl oxygens of the nanoconjugates, and the in vitro drug release profile was studied by high pressure liquid chromatography. Biocompatibility profiles of the FA-CPEG-AuNP, FA-MAP-AuNP, and FA-TAP-AuNP nanoconjugates were investigated using adult human dermal fibroblasts. Anti-breast cancer activity of 5FU-loaded nanoconjugates was investigated using MCF-7 breast cancer cells.

Results: X-ray photoelectron spectroscopy and Fourier-transform infrared spectroscopy analyses confirmed that AuNPs attached to CPEG, MAP, or TAP via the formation of π back bonding between AuNPs and the ester carbonyl group. The π back-bonded nanoconjugates exhibited sustained release of 5FU up to 27 days. FA-MAP-AuNPs exhibited an IC_{50} at 5 μg/mL, while FA-CPEG-AuNPs and FA-TAP-AuNPs showed the IC_{50} at 100 μg/mL toward MCF-7 cancer cells.

Conclusion: The developed polymer π back-bonded multifunctional gold nanoconjugates could be used as a potential drug delivery system for targeting MCF-7 cancer cells.

Keywords: polymer-gold nanoconjugates, 5-fluorouracil, anticancer activity, MCF-7 cells, green synthesis

Introduction

According to the WHO, cancer is the second leading cause of death worldwide, responsible for 8.8 million deaths in 2015 and ~70% of deaths in low- and middle-income countries.[1] Most common cancer therapies, including surgery, radiation, and chemotherapy, might cause damage to normal cells or incomplete obliteration of cancer cells. Nanotechnology is a promising method of treating cancer since it provides advanced approaches for the detection and targeting of cancer cells. Recently, gold nanoparticles (AuNPs) have received the attention of researchers due to their biocompatibility and feasibility for extensive applications in the biomedical field.[2–5]

The anticancer drug 5-fluorouracil (5FU) is one of the most commonly used drugs for treating breast cancer, and various folate (FA)-based controlled drug

Correspondence: Sengottuvelan Balasubramanian
Department of Inorganic Chemistry, University of Madras, Guindy Campus, Gandhi Mandapam Rd, Chennai, Tamil Nadu, India
Mob +91 94 4401 6707
Email bala2010@yahoo.com

Kyobum Kim
Division of Bioengineering, School of Life Sciences and Bioengineering, Incheon National University, 119 Academy-Ro, Songdo Dong, Yeonsu-gu, Incheon-22012, Republic of Korea
Tel +82 32 835 8297
Email kyobum.kim@inu.ac.kr

submit your manuscript | www.dovepress.com
Dovepress
http://dx.doi.org/10.2147/IJN.S190946

delivery systems (DDSs) have been developed to deliver 5FU to MCF-7 breast cancer cells.[6,7] Several biodegradable polymer-based materials, including gellan gum,[8] poly(D,L-lactic-co-glycolic acid),[9] polycaprolactone,[10] and L-lysine-modified hyperbranched polyester,[11] have been developed as 5FU delivery platforms to enhance the anticancer activity of 5FU. However, the size of these polymeric platforms is a major concern with regard to cell internalization of drug-incorporated carriers. Recently, metal nanoparticles (NPs), such as gold, selenium, and silver NPs, have been used as 5FU carriers to achieve efficient anticancer synergism due to their small size and ease of surface functionalization with biomolecules.[12–14]

FA receptor-mediated targeted drug delivery often focuses on breast cancer cells due to their higher surface level of FA receptor presentation compared with normal cells. As a targeting moiety, FA can be extensively conjugated with various NPs and biocompatible polymers.[15,16] Therefore, the anticancer functionality of FA-functionalized AuNPs has been extensively investigated. For instance, Mansoori et al developed FA-functionalized AuNPs by using 4-aminothiophenol and 6-mercapto-1-hexanol as a linking agent, whereas Dixit et al suggested thioctic acid-polyethylene glycol (PEG)-FA-conjugated AuNPs for targeting cancer cells.[17,18] In order to develop effective FA-based AuNP nanoconjugate platforms, two fabrication parameters are important: 1) increasing the colloidal stability of nanoconjugates by conjugating polymeric compounds and 2) covalent attachment of FA to avoid leakage of this targeting moiety before reaching cancer cells.

A green chemical synthetic method has been widely utilized to obtain biocompatible AuNPs. Green chemical synthesis of AuNPs involves the usage of water as a solvent along with biomolecules, such as amino acids, protein, carbohydrates, and phytochemicals as reducing and stabilizing agents.[2,3,5,19,20] Synthetic biocompatible polymers have also been used as stabilizing agents in the green synthesis of AuNPs.[21] Recently, multicarboxylate-PEG bifunctional copolymers, such as citrate-PEG (CPEG) copolymers were used as reducing and stabilizing agents, and the synthesized AuNPs were shown to be uniformly distributed on a CPEG copolymer matrix.[22–24]

Especially, bifunctional carboxylate-PEG polymers could play multiple roles 1) as reducing and stabilizing agents for synthesis of AuNPs and 2) as linkers for covalent attachment of FA. After synthesizing polymer-AuNPs, freely available carboxylate and hydroxyl groups of carboxylate-PEG copolymers can be used to covalently attach FA with polymer-AuNPs nanoconjugates. AuNPs can be attached to the ester carbonyl group of the polymers via formation of π back bonding between the fully filled d-orbital of AuNPs and the empty antibonding π* orbital of the ester carbonyl group of CPEG, and tartrate-PEG (TAP).[25,26] The π back-bonded ester carbonyl oxygen exhibits high electron density, which could effectively load drug molecules.[25] Hence, 5FU-loaded FA-decorated π back-bonded polymer-AuNPs nanoconjugates could exhibit sustained drug release and enhanced anticancer activity.

Therefore, in the present study, citric acid (tricarboxylic acid) was reacted with PEG to obtain a branched CPEG structure, whereas malic acid and tartaric acid (dicarboxylic acids) were reacted with PEG to obtain linear malate-PEG (MAP) and TAP structures, respectively. CPEG, MAP, and TAP were used as reducing as well as stabilizing agents for the green synthesis of CPEG-AuNP, MAP-AuNP, and TAP-AuNP (commonly referred to as polymer-AuNPs) nanoconjugates, respectively, and these AuNPs attached to polymers via the formation of π back bonding with the ester carbonyl group. Then, FA as a targeting agent was attached to the carboxylate group of the bifunctional polymer-AuNPs by carbodiimide coupling reaction to obtain FA-CPEG-AuNP, FA-MAP-AuNP, and FA-TAP-AuNP (commonly referred to as FA-polymer-AuNPs) nanoconjugates. Additionally, the chemical cancer drug 5FU was loaded onto the π back-bonded FA-polymer-AuNPs nanoconjugates. Drug-loading efficiency and in vitro 5FU release profile were evaluated by HPLC technique. Biocompatibility profiles of the FA-polymer-AuNPs nanoconjugates were investigated using adult human dermal fibroblasts (HDFs), whereas the in vitro anticancer activity of 5FU-loaded FA-polymer-AuNPs nanoconjugates was assessed using MCF-7 breast cancer cells. The drug-loading efficiencies, in vitro drug release profiles, and anticancer activities of the three different nanoconjugates with different carboxylate linkers were compared based on their chemical structure.

Materials and methods

Materials

Citric acid, malic acid, tartaric acid, stannous chloride dihydrate (Merck & Co., Inc., Whitehouse Station, NJ, USA), PEG6000 (HiMedia), Gold (III) chloride hydrate, folic acid, 5FU, 1-Ethyl-3-(3-dimethylaminopropyl) carbodiimide (EDC), and N-hydroxy succinimide (NHS) (Sigma-Aldrich Co., St Louis, MO, USA) were used without further purification. The multicarboxylate-PEG bifunctional copolymers CPEG and TAP were synthesized by direct melt polycondensation as reported in the literature.[22,25] All

solvents used were of analytical grade. The HDFs were purchased from Lonza (Walkersville, MD, USA, catalog no CC-2511), while the MCF-7 cells were purchased from American Type Culture Collection (Manassas, VA, USA, ATCC® HTB-22™), and the cells were stored in liquid nitrogen until further use.

Characterization techniques

Transmission electron microscopy (TEM) images were captured on a FEI TECNAI G2 (T-30) transmission electron microscope. The CPEG-AuNPs, MAP-AuNPs, and TAP-AuNPs were uniformly coated on aluminum foil, and X-ray photoelectron spectroscopy (XPS) spectra of the samples were recorded on an Omicron Nano Technology XPS system (XM1000) with Al-Kα radiation. The XPS data were calibrated with respect to C 1s core level peak. Fourier-transform infrared spectroscopy (FTIR) spectra were recorded on a Perkin-Elmer FTIR spectrometer. The 5FU drug was quantified by Agilent reverse phase HPLC system with C18 column by using a mixture of phosphate buffer (1 mM): acetonitrile (95:5) (pH 5.5) as a mobile phase at a flow rate of 1 mL/min at 25°C. The live/dead cell images were captured on a Nikon fluorescence microscope.

Synthesis of PEG-malate copolymer (MAP)

MAP was synthesized by direct melt polycondensation of malic acid and PEG6000. Malic acid (1 g), PEG6000 (10 g), and stannous chloride dihydrate (10 g) (0.1 wt %; 0.11 g) were taken in a round-bottom (RB) flask and degassed for 30 minutes. Then the reaction was carried out at 160°C for 3 hours under 15–25 mmHg vacuum and then cooled to room temperature. The product was dissolved in chloroform and precipitated in ice-cold diethyl ether. Then it was washed three times with diethyl ether and dried under vacuum overnight. (Yield: 7.5 g; 68.1%). (mp=46°C–48°C; FTIR: 3,445 cm^{-1}, 2,887 cm^{-1}, 1,734 cm^{-1}; ^{1}H-NMR ($CDCl_3$): δ2.8 (s), δ3.4 (s), δ3.7(s), [η]=0.25 dL/g; $\overline{Mn}$=1,858 g/mol, $\overline{Mw}$=2,125 g/mol, PDI=1.2).

General method for green synthesis of AuNPs using CPEG, MAP, and TAP

The AuNPs have been synthesized by following the literature procedure with slight modification.[22] The aqueous solution (1% wt/v) of the polymers CPEP (or) MAP or TAP and an aqueous solution of auric chloride (0.5 mM) were prepared in Millipore water. The polymer (CPEG or MAP or TAP) solutions (50 mL) were taken in three different RB flasks and pH of the solutions was adjusted to 8.5. Then, the polymer solutions were heated to 80°C under magnetic stirring. The auric chloride solution (25 mL; 0.5 mM) was added rapidly to each hot solution of polymers and stirred magnetically for 15 minutes. Then, the yellow color of the solution changed to wine-red, indicating the formation of AuNPs.

Attachment of folic acid with di- (or) tri-carboxylate-PEG-gold nanoconjugates

The folic acid was attached with polymer-AuNPs via EDC/NHS coupling reaction as shown in Figure 1A. Briefly, 75 mL of CPEG-AuNPs or MAP-AuNPs or TAP-AuNPs were taken in three different 250 mL RB flasks separately and the flasks were protected from light. The FA (5 mmol; 100 mL), NHS (5 mmol; 100 mL), and EDC (5 mmol; 100 mL) solutions were prepared separately in PBS. The prepared solutions of FA (5 mmol; 25 mL), EDC (5 mmol; 25 mL), and NHS (5 mmol; 25 mL) were added to each flask containing the polymer-AuNPs solution and stirred magnetically for 12 hours. The solutions were centrifuged at 10,000 rpm and washed with distilled deionized (DD) water to remove the free FA. The washing and centrifugation were repeated for at least three times. Finally, the nanoconjugates were freeze dried for 2 days. The FA attached CPEG-AuNPs, MAP-AuNPs, and TAP-AuNPs were abbreviated as FA-CPEG-AuNPs, FA-MAP-AuNPs, and FA-TAP-AuNPs, respectively.

Loading of 5FU on to FA-polymer-AuNPs nanoconjugates

Three types of FA-polymer-AuNPs nanoconjugates (FA-CPEG-AuNPs or FA-MAP-AuNPs or FA-TAP-AuNPs) (100 mg) were dispersed in 6 mL of DD water, and 5FU (25 mg) in 10 mL of ethanol was added to the nanoconjugates solution. The mixture was ultra-sonicated by using a probe ultrasonicator (Sonopuls, Bandelin, Berlin, Germany) for 2 minutes and stirred magnetically for 24 hours. Any unloaded free 5FU was removed by dialysis (molecular weight cut-off [MWCO] =2,000) against DD water (1 L) for 24 hours and the drug-loaded FA-polymer-AuNPs nanoconjugates were recovered by freeze drying. The free drug present in the supernatant of dialysis was determined by reverse phase HPLC technique to calculate drug-loading efficiency and percentage drug content of the FA-polymer-AuNPs nanoconjugates as given below.

$$\text{Drug loading efficiency (\%)} = \frac{-\left(\text{Amount of 5FU present in the supernatant}\right)}{\left(\text{Initial feeding amount of 5FU}\right)} \times 100$$

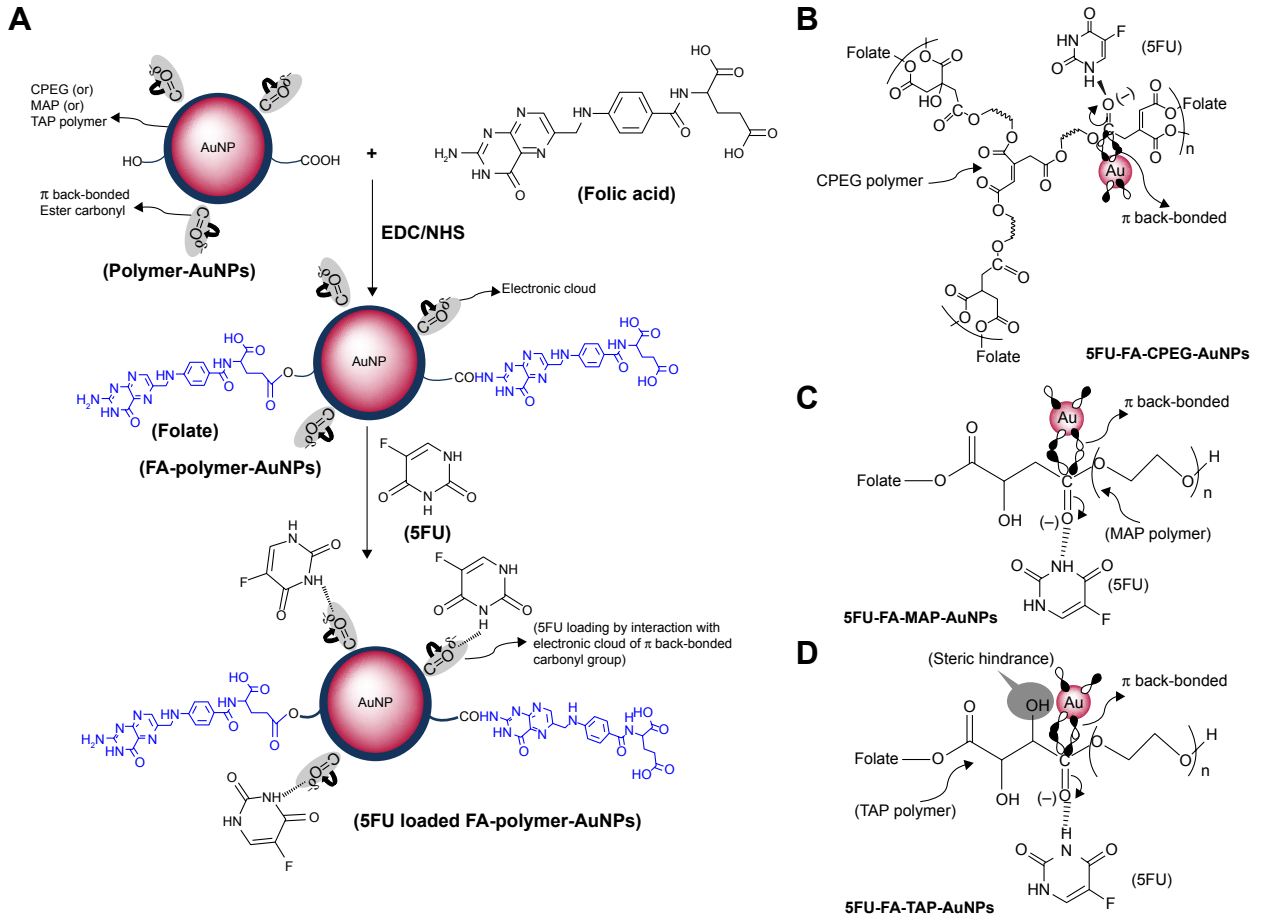

Figure 1 (**A**) General scheme of synthesis of 5FU-loaded FA-polymer-AuNP nanoconjugates, graphical representation of (**B**) 5FU-loaded FA-CPEG-AuNP, (**C**) 5FU-loaded FA-MAP-AuNP, and (**D**) 5FU-loaded FA-TAP-AuNP nanoconjugates.

Abbreviations: AuNP, gold nanoparticles; CPEG, citrate polyethylene glycol; EDC, 1-Ethyl-3-(3-dimethylaminopropyl) carbodiimide; FA, folate; 5FU, 5-fluorouracil; MAP, malate polyethylene glycol; NHS, N-hydroxy succinimide; TAP, tartrate polyethylene glycol.

$$\text{Drug content (\%)} = \frac{-\left(\text{Amount of 5FU present in the supernatant}\right)}{\left(\text{Total amount of drug loaded particles}\right)} \times 100.$$

In vitro drug release

The drug-loaded FA-polymer-AuNPs nanoconjugates (5 mg) were dispersed in 2 mL of PBS (pH 7.4), packed in a dialysis bag (MWCO=2,000) and immersed in PBS (25 mL) at 37°C under magnetic stirring.[27] The amount of drug released at different time intervals in the release medium was determined by reverse phase HPLC technique. All the experiments were carried out in triplicates and the average cumulative percentage of drug release was plotted against time.

In vitro cytotoxicity of nanoconjugates on HDFs

Biocompatibility of FA-polymer-AuNPs (FA-CPEG-AuNPs or FA-MAP-AuNPs or FA-TAP-AuNPs) nanoconjugates were investigated on HDFs. HDFs were cultured in normal growth media (DMEM) (Corning Inc., Corning, NY, USA) (89%, v/v), FBS (Corning) (10%, v/v) and penicillin–streptomycin solution (Corning) (1%) at 37°C in a humidified atmosphere of 5% CO_2. The HDFs (4,000 cells/well) were seeded in a 96-well culture plate and incubated for 24 hours at 37°C in a humidified atmosphere of 5% CO_2. After 24 hours of cell seeding, 0 (control), 5, 25, 50, 100, and 200 µg/mL of FA-polymer-AuNPs were administrated to different concentration groups. After day 1, 3, and 5 of sample treatment, cell viability was assessed by WST-1 assay (EZ-Cytox cell viability assay kit, DAEIL Lab Service, Korea) and live and dead (L/D) staining methods. To perform WST-1 assay, old media were removed from each well and the cells were washed with PBS. The cells were treated with 100 µL of the WST-1 assay solution and incubated at 37°C for 3 hours under dark condition. Then, OD of the solution was measured at 440 nm and % cell viability was calculated with respect to OD value of the control group. The L/D fluorescence

staining was performed by adding fluorescent dye solution (100 µL) containing 2 µM of Calcein-AM (Thermo scientific, Chelmsford, MA, USA) and 4 µM ethidium homodimer-1 (Thermo scientific) to the cells. After 30 minutes, the cells were monitored under a fluorescent microscope (Nikon Ti-E).

In vitro anticancer activity of drug-loaded nanoconjugates on MCF-7 cells

MCF-7 cells were cultured in DMEM (Corning) (89%, v/v), FBS (Corning) (10%, v/v) and penicillin–streptomycin solution (Corning) (1%) at the standard culture condition mentioned in previous section. The MCF-7 cells (5,000 cells/well) were seeded in 96-well culture plate and incubated for 24 hours at standard culture condition. After 24 hours of cell seeding, 5, 25, 50, 100, and 200 µg/mL of 5FU-loaded FA-CPEG-AuNPs, FA-MAP-AuNPs, and FA-TAP-AuNPs were applied separately to MCF-7 cells. In addition, free 5FU with the same concentrations were also added to MCF-7 cells and analyzed simultaneously for comparison. After day 1 and 3, cell viability was evaluated using the WST-1 assay by comparison with the OD of untreated control group and L/D fluorescence staining, as mentioned in the previous section In vitro cytotoxicity of nanoconjugates on HDFs.

Statistical analysis

The results of in vitro cellular cytotoxicity were statistically analyzed by one-way ANOVA and Tukey's multiple-comparison test by using GraphPad PRISM software (GraphPad software Inc., San Diego, CA, USA). $P<0.05$ indicates a significant difference between experimental groups. The cell viability values are plotted as mean ± standard error mean.

Results and discussion

Synthesis of FA-polymer-AuNP nanoconjugates

CPEG showed a branched structure while MAP and TAP exhibited linear structures (Figure 1B–D). All three polymers contained hydroxyl and carboxylic acid groups and thus could effectively act as reducing agents for the synthesis of AuNPs, similar to a citrate-based mechanism.[22] These polymers also acted as stabilizing agents via the formation of π back bonding between the fully filled d-orbital of AuNPs and the empty antibonding π* orbital of the ester carbonyl group to obtain spherical AuNPs with a diameter of 5–15 nm (Figure 1B–D).[26] Freely available terminal carboxylate groups of polymers were then used to attach FA via an EDC/NHS coupling reaction to obtain FA-CPEG-AuNPs, FA-MAP-AuNPs, and FA-TAP-AuNPs. Due to π back bonding, π electrons partially moved toward the carbonyl oxygen, and these electrons effectively loaded the drug molecules (Figure 1B–D).

Characterization of polymer-gold nanoconjugates

TEM analysis

The TEM image of CPEG-AuNPs indicates that the NPs exhibited a spherical shape with a uniform distribution in the CPEG polymer matrix (Figure 2A). The particle size distribution curve of CPEG-AuNPs indicates that the average diameter of AuNPs was about 9 nm (Figure 2D). Morphology of MAP-AuNPs also indicated the spherical structure of AuNPs with an average size of 11 nm (Figure 2B and E). The TEM image of TAP-AuNPs indicates that two (or) three spherical shaped AuNPs were nucleated (Figure 2C), and the average diameter of TAP-AuNPs was 14 nm (Figure 2F). TEM analysis clearly indicated that the CPEG, MAP, and TAP systems acted as effective reducing as well as stabilizing agents. The hyperbranched structure of CPEG polymer could be seen in the TEM image of CPEG-AuNPs (Figure 2A), which shows that the AuNPs were uniformly distributed on the CPEG molecule.

The energy dispersive X-ray (EDX) spectra confirm the presence of C, O, and Au atoms at 0.3, 0.6, and 2.2 keV, respectively in CPEG-AuNPs, TAP-AuNPs, and MAP-AuNPs (Figure 2G–I). Since, the samples were coated on an aluminum foil to record the EDX spectra, all the samples exhibit a signal at 1.5 keV corresponding to Al atom in addition to the signals of C, O, and Au atoms (Figure 2G–I).

X-ray photoelectron spectral analysis

Conjugation of AuNP with CPEG, MAP, and TAP polymers was confirmed by XPS technique. As shown in Figure 3, XPS data confirmed the presence of C, O, and Au atoms in all three systems. The high-resolution XPS components were de-convoluted into multiple components to elucidate the various types of conjugation present in the nanoconjugates. The C 1s XPS traces of CPEG-AuNPs exhibited four components (Figure 3A1). The peaks appearing at 285 and 286.3 eV were assigned to the C–C/C–H carbons and C–O–C carbons, respectively, whereas the peak at 288.1 eV was assigned to the carbonyl carbon. The peak at 291 eV was attributed to the shake-up component of the π–π* transition of the C=C bond present in the CPEG molecule.[26] The O 1s XPS traces of CPEG-AuNPs were de-convoluted into three components (Figure 3B1), and the peaks at 532.6 and 534.3 eV were assigned to the carbonyl oxygen (–C=O) and ethereal oxygen (C–O–C), respectively, whereas the peak at 531.3 eV

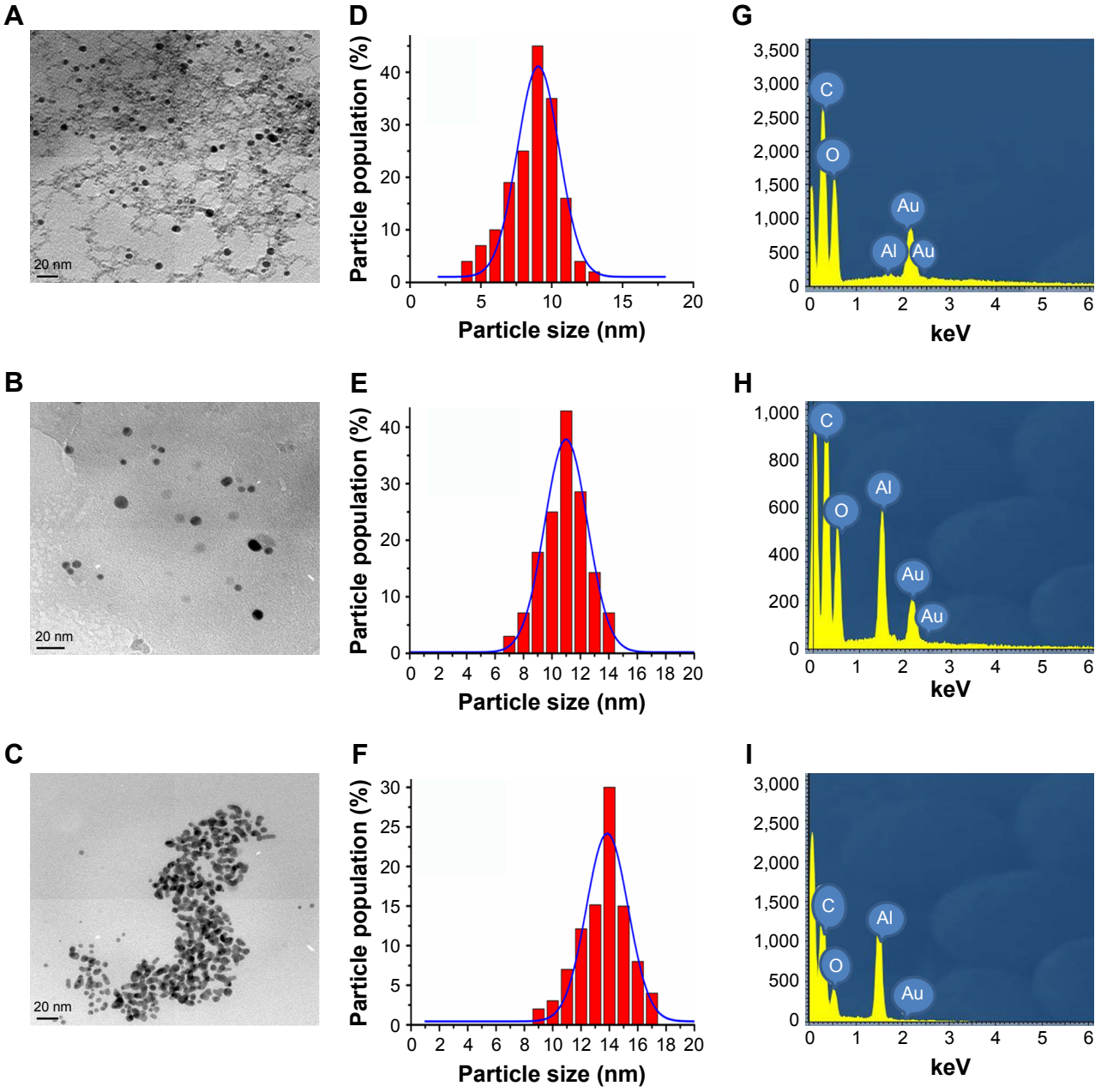

Figure 2 Transmission electron microscopy images of (**A**) CPEG-AuNPs, (**B**) MAP-AuNPs, and (**C**) TAP-AuNPs, (scale bar=20 nm), particle size distribution curves of (**D**) CPEG-AuNPs, (**E**) MAP-AuNPs, and (**F**) TAP-AuNPs, EDX spectra of (**G**) CPEG-AuNPs, (**H**) MAP-AuNPs, and (**I**) TAP-AuNPs.
Abbreviations: AuNP, gold nanoparticles; CPEG, citrate polyethylene glycol; EDX, energy dispersive X-ray; MAP, malate polyethylene glycol; TAP, tartrate polyethylene glycol.

was assigned to the carbonyl oxygen (–C=O), which was conjugated with the AuNPs.[26] The Au4f XPS trace exhibited $Au4f_{7/2}$ at 83.9 eV and $Au4f_{5/2}$ at 87.5 eV, indicating that the values were 0.2 eV higher than that of pure Au^0 (Figure 3C1). Conjugation of Au with the –C=O group was not due to Au–O sigma bonding, whereas it could be explained by the formation of π back bonding between the filled dπ or hybrid dpπ orbital of Au^0 and the empty pπ* orbital of the –C=O group (Figure S1). The –C=O group contains vacant p orbitals, which can accept the electron cloud from the filled d orbitals of Au^0 to initiate π back bonding. Hence, the high electron density of Au^0 is delocalized onto the low-lying p orbitals of –CO.[26,28] Patnaik et al reported π back bonding between Au^0 and the carbonyl group of polycarbonate films.[26] The aforementioned results confirm the conjugation of AuNPs with the CPEG polymer moiety via π back bonding, which induced stabilization of AuNPs.

In the case of MAP-AuNPs, the C 1s XPS traces exhibited three types of carbons (Figure 3A2). The C–C/C–H carbons appeared at 285 eV while the C–O–C carbon appeared

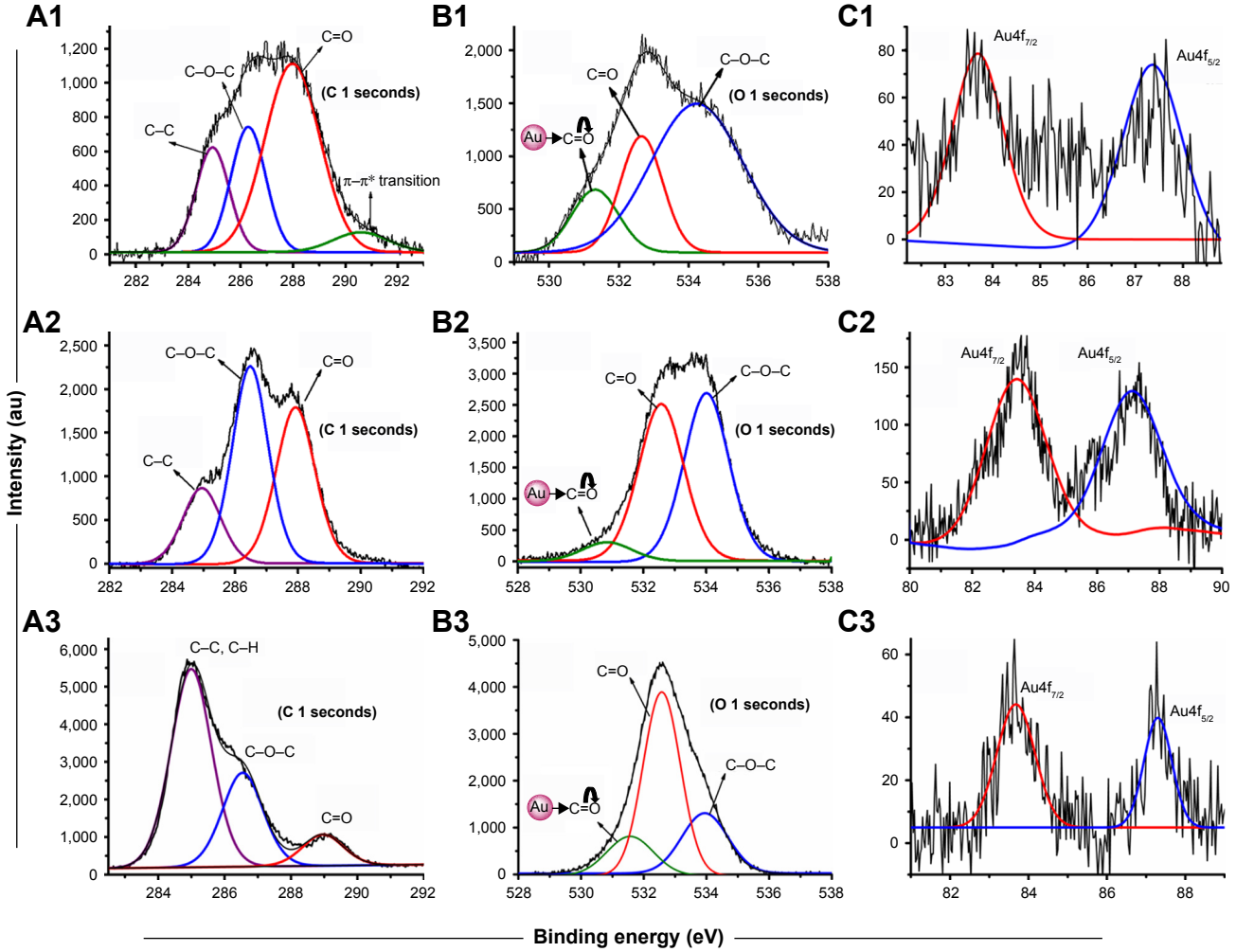

Figure 3 XPS traces of (**A1**) C 1s, (**B1**) O 1s and (**C1**) Au4f of CPEG-AuNPs, (**A2**) C 1s, (**B2**) O 1s and (**C2**) Au4f of MAP-AuNPs, and (**A3**) C 1s, (**B3**) O 1s and (**C3**) Au4f of TAP-AuNPs nanoconjugates.

Abbreviations: AuNP, gold nanoparticles; CPEG, citrate polyethylene glycol; MAP, malate polyethylene glycol; TAP, tartrate polyethylene glycol; XPS, X-ray photoelectron spectroscopy.

at 286.5 eV and the carbonyl carbon (–C=O) appeared at 287.9 eV.[26] The O 1s trace was de-convoluted into three components (Figure 3B2). Two components appeared at 532.5 and 534 eV, which were assigned to the –C=O and C–O–C oxygens, respectively, whereas the peak at 530.8 eV was assigned to the AuNP-conjugated carbonyl group via dative back bonding as discussed earlier with regard to the O 1s XPS traces of CPEG-AuNPs.[26] The Au4f XPS trace of MAP-AuNPs also exhibited an $Au4f_{7/2}$ signal at 83.9 eV and $Au4f_{5/2}$ signal at 87.5 eV (Figure 3C2).

In the case of TAP-AuNPs, C 1s of C–C/C–H appeared at 284.9 eV, C 1s traces of C–O–C appeared at 286.5 eV, and C 1s traces of –C=O appeared at 289 eV (Figure 3A3). The O 1s XPS traces were fitted to three components, including MAP-AuNPs and CPEG-AuNPs (Figure 3B3). The peak at 532.6 eV was assigned to the –C=O oxygen while the peak at 533.9 eV was assigned to the C–O–C oxygen trace.[26] The π back-bonded carbonyl oxygen trace appeared at 351.3 eV. These XPS results confirm the conjugation of AuNPs via formation of π back bonding with the ester carbonyl oxygens of CPEG, MAP, and TAP polymers.

FTIR spectral analysis of drug-loaded nanoconjugates

FTIR spectral analysis was carried out to characterize chemical conjugation in each fabrication step as well as 5FU drug loading on FA-polymer-AuNP nanoconjugates. The CPEG, MAP, and TAP polymers exhibited ester carbonyl stretching frequencies at 1,735 cm^{-1}, 1,739 cm^{-1}, and 1,744 cm^{-1}, respectively (Figure 4A, E and I), and these values shifted to lower frequency regions at 1,640 cm^{-1}, 1,592 cm^{-1}, and 1,610 cm^{-1}, respectively, after conjugation with AuNPs.[25] These results confirm the formation of π back bonding between AuNPs and the ester carbonyl group. Due to the

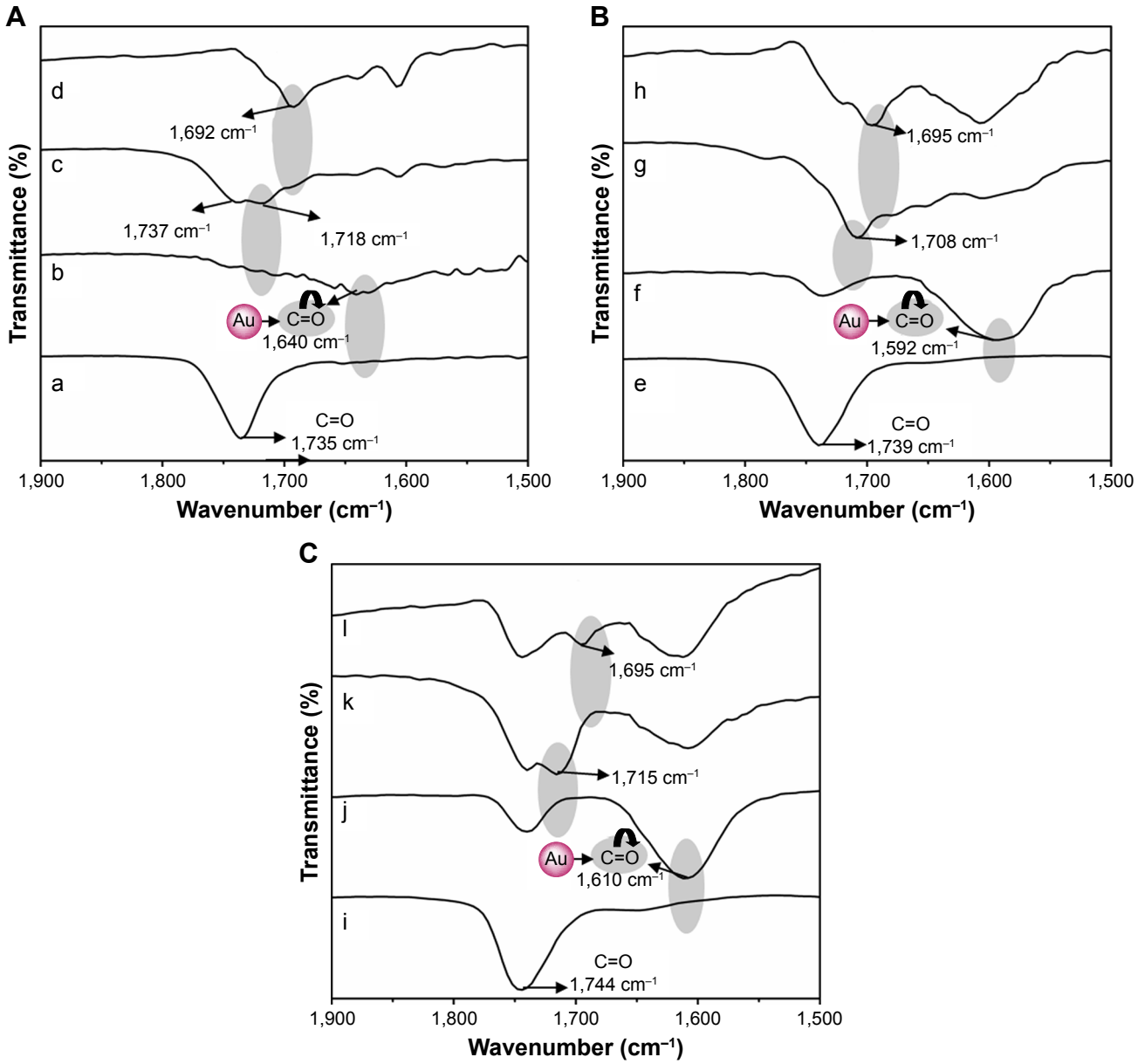

Figure 4 FTIR spectra of (**A**) CPEG polymer-based nanoconjugates: (a) CPEG, (b) CPEG-AuNPs, (c) FA-CPEG-AuNPs, and (d) 5FU-loaded FA-CPEG-AuNPs, (**B**) MAP polymer-based nanoconjugates: (e) MAP, (f) MAP-AuNPs, (g) FA-MAP-AuNPs, and (h) 5FU-loaded FA-MAP-AuNPs, and (**C**) TAP polymer-based nanoconjugates: (i) TAP, (j) TAP-AuNPs, (k) FA-TAP-AuNPs, and (l) 5FU-loaded FA-TGA-AuNPs.

Abbreviations: AuNP, gold nanoparticles; CPEG, citrate polyethylene glycol; FA, folate; 5FU, 5-fluorouracil; FTIR, Fourier-transform infrared spectroscopy; MAP, malate polyethylene glycol; TAP, tartrate polyethylene glycol; TGA, thioglycolic acid.

formation of π back bonding, the carbonyl double bond character became weak, and thus the carbonyl stretching frequencies of CPEG-AuNPs, MAP-AuNPs, and TAP-AuNPs shifted 95–147 cm^{-1} lower compared with AuNP-free polymers (Figure 4B, F and J). Behera et al similarly reported that AuNP-attached poly(vinylpyrrolidone) (PVP) exhibited a carbonyl stretching frequency that was 5 cm^{-1} lower than that of AuNP-free PVP.[29] After attachment of FA, FA-CPEG-AuNP, FA-MAP-AuNP, and FA-TAP-AuNP nanoconjugates exhibited distinct signals at 1,718 cm^{-1}, 1,708 cm^{-1}, and 1,715 cm^{-1}, respectively, due to the amide or acid carbonyl group of FA, confirming attachment of FA to the polymer-AuNP nanoconjugates.[30] Finally, 5FU-loaded FA-CPEG-AuNP, FA-MAP-AuNP, and FA-TAP-AuNP nanoconjugates exhibited distinct signals at 1,692 cm^{-1}, 1,695 cm^{-1}, and 1,695 cm^{-1}, respectively, compared with drug-free nanoconjugates, and this observation could be due to the overlapping carbonyl stretching frequencies of 5FU and FA molecules (Figure 4D, H and L). These results confirm the sequential fabrication of FA-thioglycolic acid (TGA)-AuNPs as well as the further incorporation of 5FU into the nanoconjugates (Figure 4C, G and K).

In vitro drug release profile

The 5FU loading efficiency and in vitro drug release profile of 5FU-loaded FA-polymer-AuNP nanoconjugates were determined by reverse-phase HPLC technique. The drug-loading efficiencies and percentage drug contents are shown in Table 1. The nanoconjugates obtained with linear polymer structures (FA-MAP-AuNPs and FA-TAP-AuNPs) exhibited relatively higher 5FU loading efficiencies than that of nanoconjugates obtained with a branched polymer structure (FA-CPEG-AuNPs). FA-MAP-AuNP nanoconjugates exhibited a relatively higher drug-loading efficiency compared with FA-TAP-AuNP nanoconjugates. The presence of two hydroxyl groups adjacent to both carbonyl groups of the tartrate moiety in the FA-TAP-AuNP system could have added steric hindrance to the 5FU drug molecules at the π back-bonded ester carbonyl group (Figure 1D), resulting in relatively lower drug-loading efficiencies compared with the FA-MAP-AuNP system.

In vitro drug release profiles show that the 5FU-loaded FA-CPEG-AuNP, FA-MAP-AuNP, and FA-TAP-AuNP nanoconjugates exhibited 22.6%, 19.3%, and 39.6%, respectively, sustained drug release up to 27 days (Figure 5). The 5FU-loaded FA-TAP-AuNPs system exhibited faster 5FU release compared with the other two systems. This result suggests that the steric hindrance experienced by the two hydroxyl groups adjacent to the two π back-bonded ester carbonyls in the FA-TAP-AuNP nanoconjugates could have induced faster 5FU release. Since the citrate and malate moieties each possessed one hydroxyl group adjacent to only one ester carbonyl group, the other ester carbonyl groups of the citrate and malate moieties were free from any steric hindrance. Hence, the FA-CPEG-AuNP and FA-MAP-AuNP nanoconjugates with lesser steric hindrance exhibited slower 5FU release profiles irrespective of a linear or branched structure. These results strongly suggest that the steric hindrance experienced by the hydroxyl group near the π back-bonded ester carbonyl group affected both the drug-loading efficiency and in vitro drug release properties of the nanoconjugates, whereas the type of polymer (linear or branched) had a remarkable effect on drug-loading efficiency.

Table 1 Drug-loading efficiency and drug content percentage values of 5FU-loaded nanoconjugates

Samples	Drug-loading efficiency (%)	Drug content (%)
5FU-FA-CPEG-AuNPs	8.6	2.1
5FU-FA-MAP-AuNPs	29.1	6.8
5FU-FA-TAP-AuNPs	9.9	2.4

Abbreviations: AuNP, gold nanoparticles; CPEG, citrate polyethylene glycol; FA, folate; 5FU, 5-fluorouracil; MAP, malate polyethylene glycol; TAP, tartrate polyethylene glycol.

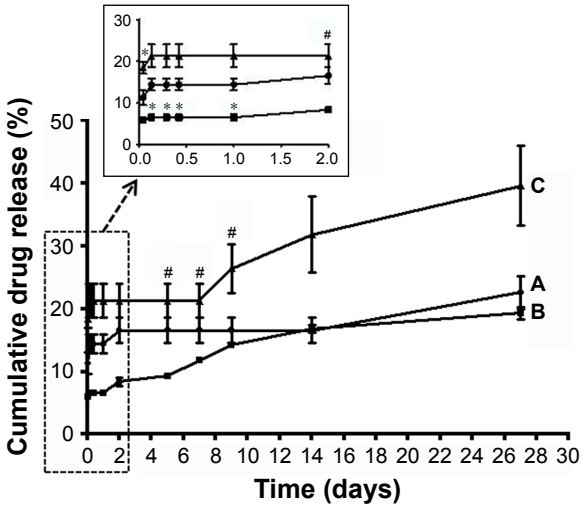

Figure 5 In vitro cumulative 5FU release profiles of (**A**) FA-CPEG-AuNPs, (**B**) FA-MAP-AuNPs, and (**C**) FA-TAP-AuNPs nanoconjugate.
Note: *significantly different from CPEG-FA-AuNPs, #significantly different from FA-MAP-AuNPs.
Abbreviations: AuNP, gold nanoparticles; CPEG, citrate polyethylene glycol; FA, folate; 5FU, 5-fluorouracil; MAP, malate polyethylene glycol; TAP, tartrate polyethylene glycol.

Recently, Safwat et al reported that 5FU-loaded cetyltrimethyl ammonium bromide (CTAB)-coated AuNPs (5FU/CTAB-AuNPs) exhibited in vitro drug release only up to 24 hours and that incorporation of 5FU/CTAB-AuNPs into Pluronic F127 gel sustained the rate of drug release.[27] Safwat et al also reported that 5FU-loaded TGA-capped AuNPs and glutathione-capped AuNPs exhibited pH-responsive in vitro drug release profiles, although drug release was completed within 12 hours.[12] In addition, Duan et al reported that 5FU-loaded poly(lactic acid–4-hydroxyproline–polyethylene glycol) NPs showed an initial burst release of 5FU (~60%) up to 24 hours, followed by sustained 5FU release >90 hours.[31] These results indicate that biodegradable polymer-based drug carriers exhibited sustained 5FU release over a relatively longer duration, whereas polymer-free AuNPs carriers maintained 5FU release only for a short period. Interestingly, in the present study, our FA-CPEG-AuNPs, FA-MAP-AuNPs, and FA-TAP-AuNPs exhibited sustained 5FU release up to 27 days (Figure 5) possibly due to the strong interaction between 5FU and the π back-bonded ester carbonyl groups of the nanoconjugates.

In vitro biocompatibility test

Biocompatibility of the developed drug-free FA-polymer-AuNP nanoconjugates was assessed using HDFs. The in vitro cytotoxicity results show that all three FA-polymer-AuNP systems exhibited >95% cellular viability up to 200 μg/mL over a period of 5 days compared with the control group (ie, nanoconjugates-free HDFs group) (Figure S2). In the L/D fluorescence staining images, nanoconjugate-treated HDFs in all three formulations showed only live cells without any

red-colored dead cells, like the control group (Figure S3). These results demonstrate that our FA-CPEG-AuNPs, FA-MAP-AuNPs, and FA-TAP-AuNPs were highly biocompatible toward normal human cells, and thus the developed nanoconjugates could be a feasible drug delivery platform.

In vitro anticancer activity of AuNP nanoconjugates in MCF-7 cells

The anticancer activity of the 5FU-loaded FA-polymer-AuNP nanoconjugates toward MCF-7 cancer cells was assessed. The results indicate that the 5FU-FA-CPEG-AuNPs, 5FU-FA-MAP-AuNPs, and 5FU-FA-TAP-AuNPs exhibited approximately half maximal inhibitory concentrations (IC_{50}) of 100 μg/mL, 5 μg/mL, and 100 μg/mL, respectively, on day 1 (Figure 6A). All drug-loaded nanoconjugates exhibited inhibitory effects against MCF-7 proliferation after 3 days of incubation, and inhibitory activities increased with an increasing concentration of 5FU nanoconjugates (Figure 6B). The 5FU-loaded FA-MAP-AuNPs and FA-TAP-AuNPs with higher 5FU loading efficiencies exhibited better inhibitory activities at concentrations >25 μg/mL on day 3 (Figure 6B). These results indicate that the nanoconjugates with a linear polymer structure (FA-MAP-AuNPs and FA-TAP-AuNPs) inhibited proliferation of MCF-7 cells more effectively due to their higher drug-loading efficiency compared with the nanoconjugates with a branched polymer structure (FA-CPEG-AuNPs). Furthermore, all treatment groups exhibited significantly reduced MCF-7 proliferation compared with the untreated control MCF-7 group showing 100% cell viability (data not shown) on day 3. These results demonstrate that the developed FA-polymer-AuNP nanoconjugates could effectively deliver incorporated 5FU drug to the FA receptors of MCF-7 cells.

Moreover, our results demonstrate that a 5FU delivery platform could be more effective for inhibition of MCF-7 proliferation compared with conventional free 5FU delivery. For instance, Le et al reported that 5FU-loaded FA-PEG-modified nanoliposomes (5FU-FA-PEG-LPs) inhibited MCF-7 cells with IC_{50} values of 10.2 μg/mL on day 1 and 4.4 μg/mL on day 2.[6] In contrast, the IC_{50} values of free 5FU were shown to be >20 μg/mL and 17.9 μg/mL on days 1 and 2, respectively. These results indicate that the incorporation of 5FU into FA-PEG-LPs augmented anticancer functionality compared with free 5FU, specifically for MCF-7 breast cancer cells. Similarly, Abd Rabou et al developed taribavirin (TBV) and 5FU-loaded PEGylated solid lipid NPs (PEG-SLNPs) for inhibition of MCF-7 proliferation.[32] This study also observed lower IC_{50} values for TBV and 5FU incorporated into PEG-SLNPs compared with their free-drug counterparts.

Recently, polymer-stabilized metal NP-based DDSs exhibited synergistic effects on inhibition of MCF-7 cells. For instance, Matai et al reported that 5FU-loaded poly(amidoamine) (PAMAM) dendrimer-capped silver NPs (PAMAM-AgNPs) inhibited MCF-7 cells more effectively with an IC_{50} value of 1.5 μg/mL, and this synergistic effect was attributed to the combined cytotoxicity of PAMAM-AgNPs and 5FU.[14]

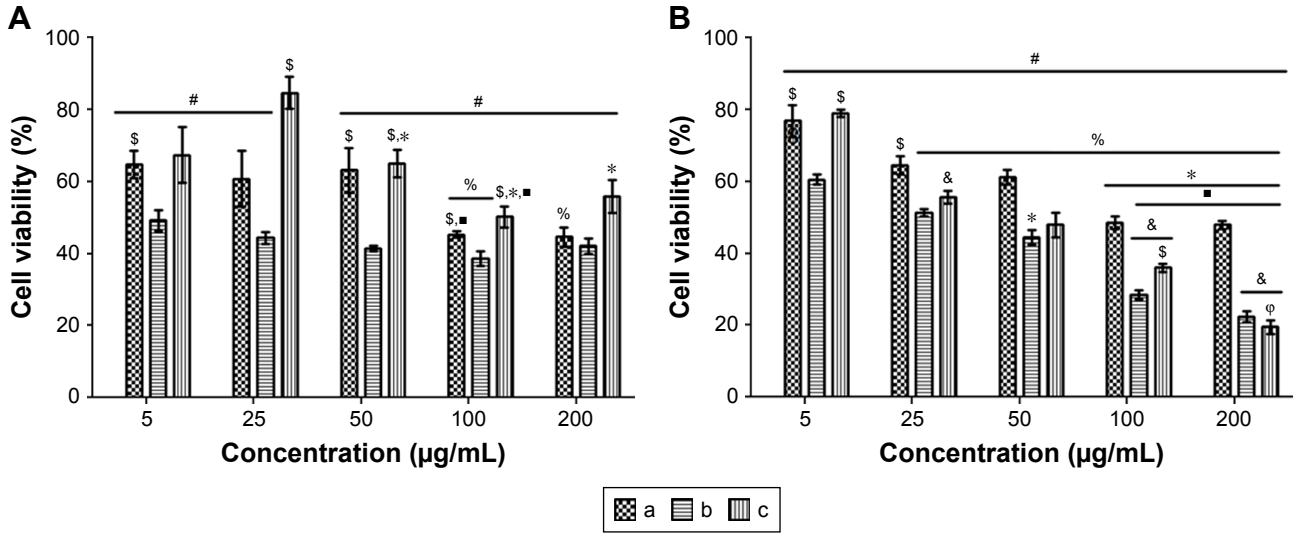

Figure 6 In vitro cytotoxicity of (**a**) 5FU-FA-CPEG-AuNPs, (**b**) 5FU-FA-MAP-AuNPs, and (**c**) 5FU-FA-TAP-AuNPs on MCF-7 cells during (**A**) day 1 and (**B**) day 3.
Notes: Statistical acronyms (#) significantly different from untreated control group (100% viability), (*) significantly different from 25 μg/mL within same group, ($) significantly different from 5FU-FA-MAP-AuNPs at same concentration, (%) significantly different from 5 μg/mL within same group, (■) significantly different from 50 μg/mL within same group, (&) significantly different from 5FU-FA-CPEG-AuNPs at same concentration and (φ) significantly different from 100 μg/mL within same group.
Abbreviations: AuNP, gold nanoparticles; CPEG, citrate polyethylene glycol; FA, folate; 5FU, 5-fluorouracil; MAP, malate polyethylene glycol; TAP, tartrate polyethylene glycol.

Interestingly, in the present study, 5FU-loaded FA-MAP-AuNP nanoconjugates exhibited an IC_{50} value of 5 µg/mL on day 1 (Figure 6A). It should be emphasized that 5 µg of 5FU-loaded FA-MAP-AuNPs contained only 335 ng of 5FU (6.7% drug content). 5FU-loaded FA-CPEG-AuNPs showed an IC_{50} value of 100 µg/mL with 2.1 µg of 5FU in the test sample (2.1% drug content) on day 1. Similarly, 5FU-loaded FA-TAP-AuNPs exhibited an IC_{50} value of 100 µg/mL with 2.4 µg of 5FU in the test sample (2.4% drug content) on day 1 (Figure 6A). All three 5FU-loaded nanoconjugates exhibited higher inhibitory activities along with lower amounts of 5FU compared with the free 5FU group on day 1 (data not shown, reported in our earlier work).[33] In particular, 5FU-FA-MAP-AuNPs with 335 ng of incorporated 5FU effectively inhibited MCF-7 cancer cells compared with 5FU-FA-PEG-LPs, TBV-loaded PEG-SLNPs, 5FU-loaded PEG-SLNPs, 5FU-loaded PAMAM-AgNPs, free TBV, and free 5FU, as reported in the literature.[6,14,32] Hence, our 5FU-loaded π back-bonded FA-polymer-AuNP nanoconjugates showed enhanced inhibitory activity along with lower 5FU drug content than administration of free 5FU, indicating that our delivery system could reduce the side effects of 5FU without compromising its anticancer functionality.

Furthermore, the L/D staining images indicate a higher number of dead MCF-7 cells in 5FU-loaded FA-polymer-AuNPs compared with the control, and FA-MAP-AuNPs showed more dead cells after days 1 and 3. (Figure 7). This observation agrees with the WST-1 assay results in

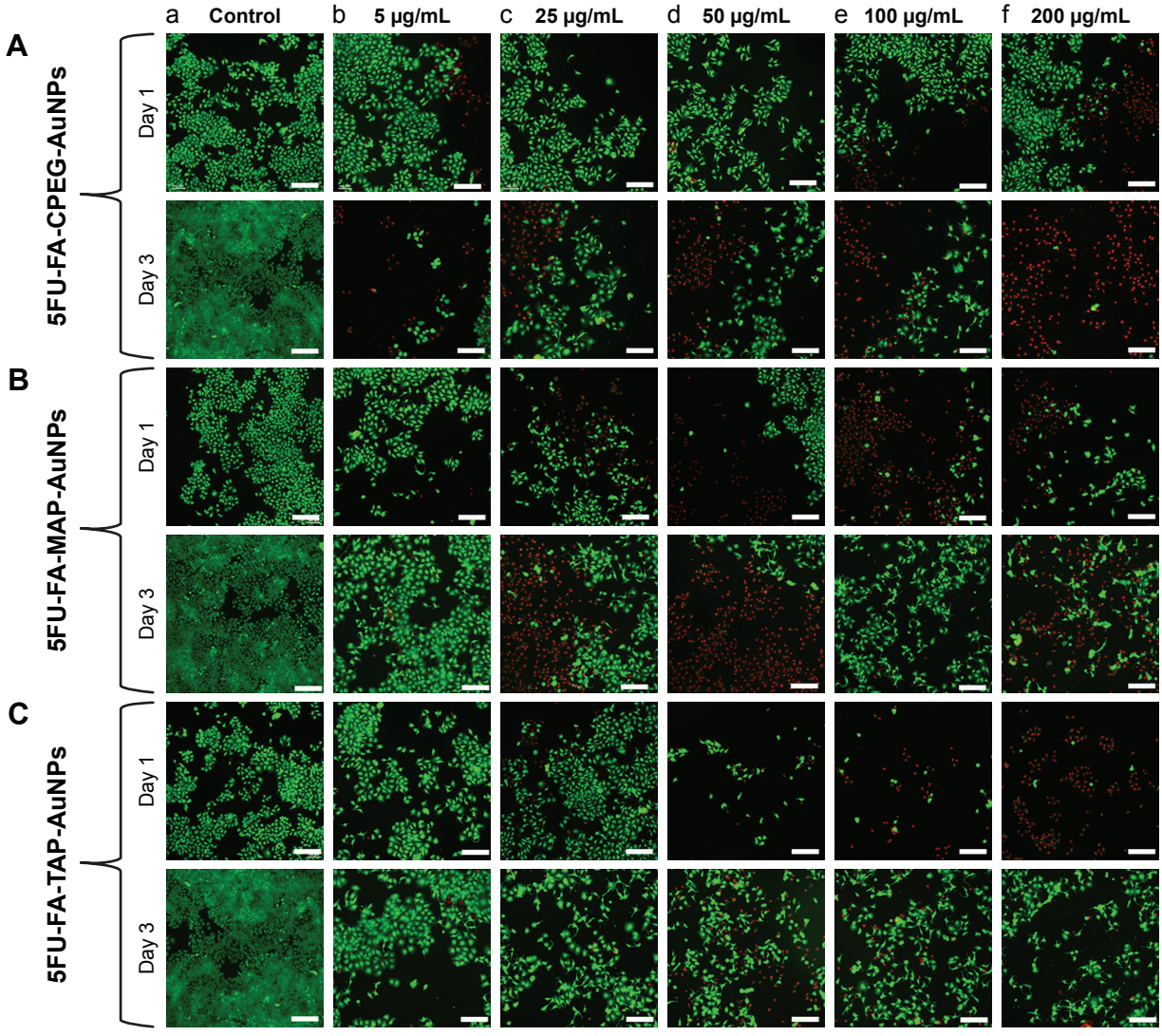

Figure 7 Live/dead fluorescent images of MCF-7 cells treated with 5FU-loaded (**A**) FA-CPEG-AuNPs, (**B**) FA-MAP-AuNPs, and (**C**) FA-TAP-AuNPs at (a) 0, (b) 5, (c) 25, (d) 50, (e) 100, and (f) 200 µg/mL after day 1 and day 3 of treatment (scale bar=200 µm).

Abbreviations: AuNP, gold nanoparticles; CPEG, citrate polyethylene glycol; FA, folate; 5FU, 5-fluorouracil; MAP, malate polyethylene glycol; TAP, tartrate polyethylene glycol.

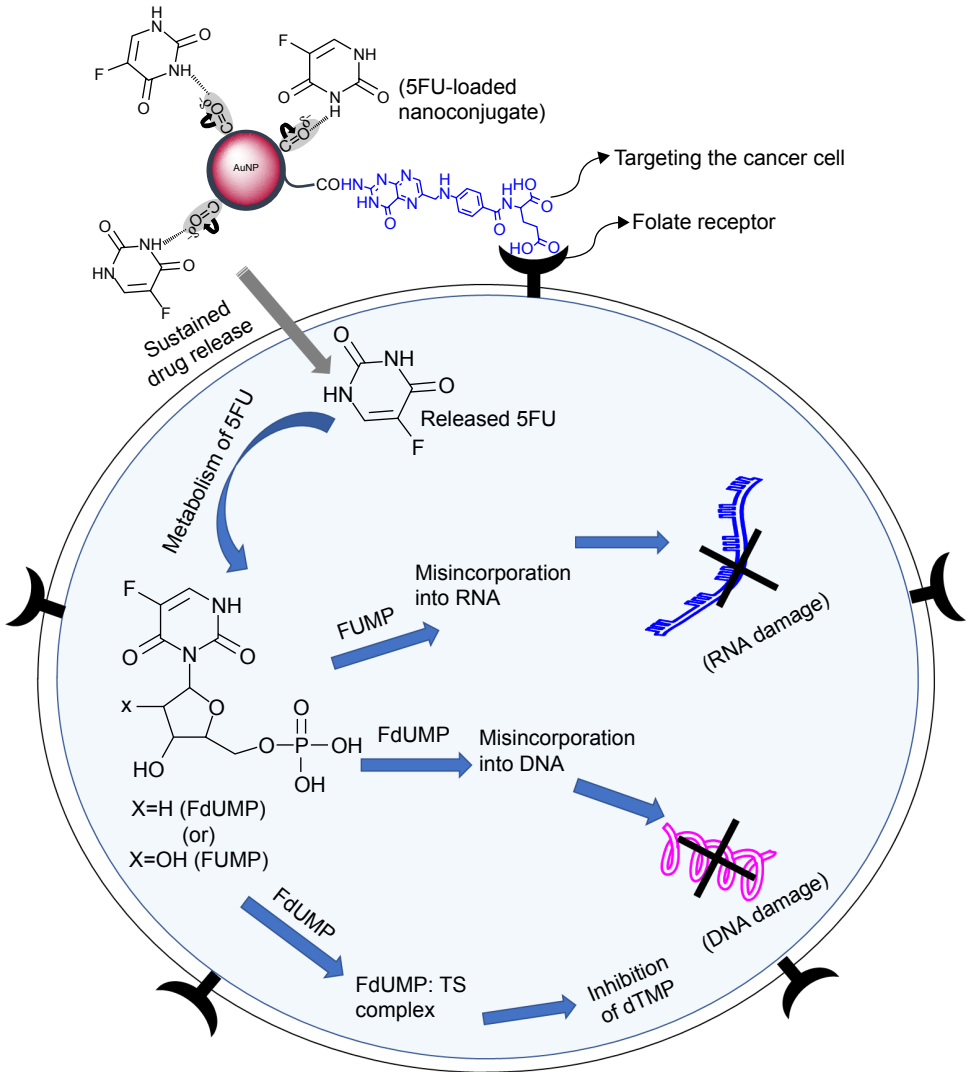

Figure 8 Mechanism of folate receptor-mediated drug targeting and inhibition of MCF-7 cancer cells by 5FU-loaded FA-polymer-AuNPs nanoconjugates.
Abbreviations: AuNP, gold nanoparticles; FdUMP, 5-fluorodeoxyuridine monophosphate; FUMP, 5-fluorouridine monophosphate; 5FU, 5-fluorouracil; TS, thymidylate synthase; dTMP, deoxythymidine monophosphate.

Figure 6. These results clearly indicate that the 5FU-loaded π back-bonded FA-polymer-AuNP nanoconjugates could effectively target and inhibit MCF-7 cancer cells even with lesser drug content, and 5FU administration with reduced side effects to patients can be anticipated.

It can be suggested that 5FU released from the FA-polymer-AuNP nanoconjugates inhibited the proliferation of MCF-7 cells by the following mechanisms: 1) inhibition of production of deoxythymidine monophosphate and 2) misincorporation of 5-fluorodeoxyuridine monophosphate with a DNA chain or incorporation of 5-fluorouridine monophosphate with an RNA chain (Figure 8).[34,35]

Conclusion

Two types of linear carboxylate-PEG polymer structures were synthesized by using malic acid and tartaric acid as a linear linker, whereas the branched carboxylate-PEG structure was obtained by using citric acid as a cross linker. All three polymers effectively acted as reducing as well as stabilizing agents for the synthesis of spherical AuNPs. The XPS and FTIR results confirm the conjugation of AuNPs with a polymer backbone via the formation of π back bonding between the fully filled d-orbital of Au^0 and the empty antibonding orbital of the ester carbonyl group. The FTIR results also confirm the attachment of FA with the polymer-AuNPs as well as loading of 5FU onto the nanoconjugates. The steric hindrance at the π back-bonded ester carbonyl group strongly affected the release properties of 5FU, and thus the 5FU-loaded FA-TAP-AuNPs with steric hindrance at both carbonyl groups of the tartrate moiety exhibited relatively faster release compared with the two other systems with lesser steric hindrance. The developed FA-CPEG-AuNP,

FA-MAP-AuNP, and FA-TAP-AuNP nanoconjugates were biocompatible toward HDFs up to 200 µg/mL for 3 days. Since the drug molecules were strongly attached onto the π back-bonded ester carbonyl group, the nanoconjugates exhibited sustained 5FU release up to 27 days. The FA-MAP-AuNPs with a linear polymer structure and higher 5FU loading efficiency inhibited proliferation of MCF-7 cells at a low concentration of 5 µg/mL compared with other systems published previously. Hence, this investigation provides a feasible platform for the development of biocompatible π back-bonded FA-polymer-AuNP nanoconjugate systems for exhibiting anti-breast cancer activity in cellular levels.

Acknowledgment

This research work was partly supported by Incheon National University Post-Doctoral Research Program (2018–2019) and Nano-Material Technology Development Program through NRF funded by the Ministry of Science and ICT (no. 2017M3A7B8061942).

Disclosure

The authors report no conflicts of interest in this work.

References

1. Ferlay J, Soerjomataram I, Dikshit R, et al. Cancer incidence and mortality worldwide: sources, methods and major patterns in GLOBOCAN 2012. *Int J Cancer*. 2015;136(5):E359–E386.
2. Kamalakannan R, Mani G, Muthusamy P, Susaimanickam AA, Kim K. Caffeine-loaded gold nanoparticles conjugated with PLA-PEG-PLA copolymer for in vitro cytotoxicity and anti-inflammatory activity. *J Ind Eng Chem*. 2017;51:113–121.
3. Reena K, Prabakaran M, Leeba B, Gajendiran M, Antony SA. Green synthesis of pectin-gold-PLA-PEG-PLA nanoconjugates: In vitro cytotoxicity and anti-inflammatory activity. *J Nanosci Nanotechnol*. 2017;17(7):4549–4557.
4. Gilam A, Conde J, Weissglas-Volkov D, et al. Local microRNA delivery targets palladin and prevents metastatic breast cancer. *Nat Commun*. 2016;7(1):12868.
5. Reena K, Balashanmugam P, Gajendiran M, Antony SA. Synthesis of leucas aspera extract loaded Gold-PLA-PEG-PLA amphiphilic copolymer nanoconjugates: in vitro cytotoxicity and anti-inflammatory activity studies. *J Nanosci Nanotechnol*. 2016;16(5): 4762–4770.
6. Le VM, Tran Nho TD, Trieu Ly H, et al. Enhanced anticancer efficacy and tumor targeting through folate-PEG modified nanoliposome loaded with 5-fluorouracil. *Adv Nat Sci Nanosci Nanotechnol*. 2017;8(1): 015008.
7. Kumar SSD, Mahesh A, Antoniraj MG, Rathore HS, Houreld NN, Kandasamy R. Cellular imaging and folate receptor targeting delivery of gum kondagogu capped gold nanoparticles in cancer cells. *Int J Biol Macromol*. 2018;109:220–230.
8. Sahoo SK, Sahoo SK, Behera A, Patil SV, Panda SK. Formulation, in vitro drug release study and anticancer activity of 5-fluorouracil loaded gellan gum microbeads. *Acta Pol Pharm*. 2013;70(1):123–127.
9. Leelakanok N, Geary SM, Salem AK. Antitumor efficacy and toxicity of 5-fluorouracil-loaded poly(lactide co-glycolide) pellets. *J Pharm Sci*. 2018;107(2):690–697.
10. Öztürk K, Mashal AR, Yegin BA, Çalış S. Preparation and *in vitro* evaluation of 5-fluorouracil-loaded PCL nanoparticles for colon cancer treatment. *Pharm Dev Technol*. 2017;22(5):635–641.
11. Bal Öztürk A, Cevher E, Pabuccuoğlu S, Özgümüş S. pH sensitive functionalized hyperbranched polyester based nanoparticulate system for the receptor-mediated targeted cancer therapy. *Int J Polym Mater Polym Biomater*. Epub 2018 Mar 11.
12. Safwat MA, Soliman GM, Sayed D, Attia MA. Gold nanoparticles enhance 5-fluorouracil anticancer efficacy against colorectal cancer cells. *Int J Pharm*. 2016;513(1–2):648–658.
13. Liu W, Li X, Wong YS, et al. Selenium nanoparticles as a carrier of 5-fluorouracil to achieve anticancer synergism. *ACS Nano*. 2012;6(8): 6578–6591.
14. Matai I, Sachdev A, Gopinath P. Multicomponent 5-fluorouracil loaded PAMAM stabilized-silver nanocomposites synergistically induce apoptosis in human cancer cells. *Biomater Sci*. 2015;3(3): 457–468.
15. Zhu Y, Fang Y, Kaskel S. Folate-Conjugated Fe3O4@SiO2 Hollow Mesoporous Spheres for Targeted Anticancer Drug Delivery. *J Phys Chem C*. 2010;114(39):16382–16388.
16. Dong S, Cho HJ, Lee YW, Roman M. Synthesis and cellular uptake of folic acid-conjugated cellulose nanocrystals for cancer targeting. *Biomacromolecules*. 2014;15(5):1560–1567.
17. Mansoori GA, Brandenburg KS, Shakeri-Zadeh A. A comparative study of two folate-conjugated gold nanoparticles for cancer nanotechnology applications. *Cancers*. 2010;2(4):1911–1928.
18. Dixit V, Van den Bossche J, Sherman DM, Thompson DH, Andres RP. Synthesis and grafting of thioctic acid−PEG−folate conjugates onto Au nanoparticles for selective targeting of folate receptor-positive tumor cells. *Bioconjug Chem*. 2006;17(3):603–609.
19. Shankar SS, Rai A, Ankamwar B, Singh A, Ahmad A, Sastry M. Biological synthesis of triangular gold nanoprisms. *Nat Mater*. 2004;3(7): 482–488.
20. Uthaman S, Kim HS, Revuri V, et al. Green synthesis of bioactive polysaccharide-capped gold nanoparticles for lymph node CT imaging. *Carbohydr Polym*. 2018;181:27–33.
21. García-Serrano J, Pal U, Herrera AM, Salas P, Ángeles-Chávez C. One-step "green" synthesis and stabilization of Au and Ag nanoparticles using ionic polymers. *Chem Mater*. 2008;20(16):5146–5153.
22. Gajendiran M, Jainuddin Yousuf SM, Elangovan V, Balasubramanian S. Gold nanoparticle conjugated PLGA–PEG–SA–PEG–PLGA multiblock copolymer nanoparticles: synthesis, characterization, in vivo release of rifampicin. *J Mater Chem B*. 2014;2(4):418–427.
23. Tavakoli Naeini A, Vossoughi M, Adeli M. Simultaneously synthesis and encapsulation of metallic nanoparticles using linear–dendritic block copolymers of poly(ethylene glycol)-poly(citric acid). *Key Eng Mater*. 2011;478:7–12.
24. Tavakoli Naeini A, Adeli M, Vossoughi M. Synthesis of gold nanoparticle necklaces using linear–dendritic copolymers. *Eur Polym J*. 2010; 46(2):165–170.
25. Gajendiran M, Balashanmugam P, Kalaichelvan PT, Balasubramanian S. Multi-drug delivery of tuberculosis drugs by π-back bonded gold nanoparticles with multiblock copolyesters. *Mater Res Express*. 2016;3(6): 065401.
26. Patnaik A, Li C. Evidence for metal interaction in gold metallized polycarbonate films: an x-ray photoelectron spectroscopy investigation. *J Appl Phys*. 1998;83(6):3049–3056.
27. Safwat MA, Soliman GM, Sayed D, Attia MA. Fluorouracil-loaded gold nanoparticles for the treatment of skin cancer: development, *in vitro* characterization, and *in vivo* evaluation in a mouse skin cancer xenograft model. *Mol Pharm*. 2018;15(6):2194–2205.
28. Tripathy P, Mishra A, Ram S, Fecht HJ, Bansmann J, Behm RJ. X-ray photoelectron spectrum in surface Interfacing of gold nanoparticles with polymer molecules in a hybrid nanocomposite structure. *Nanotechnology*. 2009;20(7):075701.
29. Behera M, Ram S. Spectroscopy-based study on the interaction between gold nanoparticle and poly(vinylpyrrolidone) molecules in a non-hydrocolloid. *Int Nano Lett*. 2013;3(1):17.
30. Li G, Li D, Zhang L, Zhai J, Wang E. One-step synthesis of folic acid protected gold nanoparticles and their receptor-mediated intracellular uptake. *Chemistry*. 2009;15(38):9868–9873.

31. Duan J, Du J, Zheng YB. Preparation and drug-release behavior of 5-fluorouracil-loaded poly(lactic acid–4-hydroxyproline–polyethylene glycol) amphipathic copolymer nanoparticles. *J Appl Polym Sci*. 2007; 103(4):2654–2659.
32. Abd-Rabou AA, Bharali DJ, Mousa SA. Taribavirin and 5-fluorouracil-loaded pegylated-lipid nanoparticle synthesis, p38 docking, and antiproliferative effects on MCF-7 breast cancer. *Pharm Res*. 2018;35(4):76.
33. Mani G, Kim S, Kim K. Development of folate-thioglycolate-gold nanoconjugates by using citric acid-peg branched polymer for inhibition of MCF-7 cancer cell proliferation. *Biomacromolecules*. 2018;19(8): 3257–3267.
34. Weiss JT, Dawson JC, Macleod KG, et al. Extracellular palladium-catalysed dealkylation of 5-fluoro-1-propargyl-uracil as a bioorthogonally activated prodrug approach. *Nat Commun*. 2014;5(1): 3277.
35. Zhang N, Yin Y, Xu SJ, Chen WS. 5-fluorouracil: mechanisms of resistance and reversal strategies. *Molecules*. 2008;13(8):1551–1569.

Supplementary materials

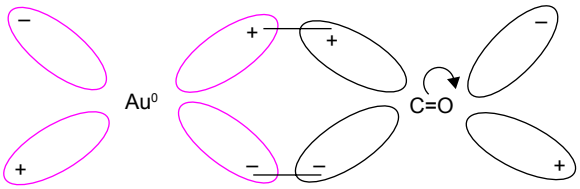

Figure S1 Schematic representation of Au-CO π back bonding.

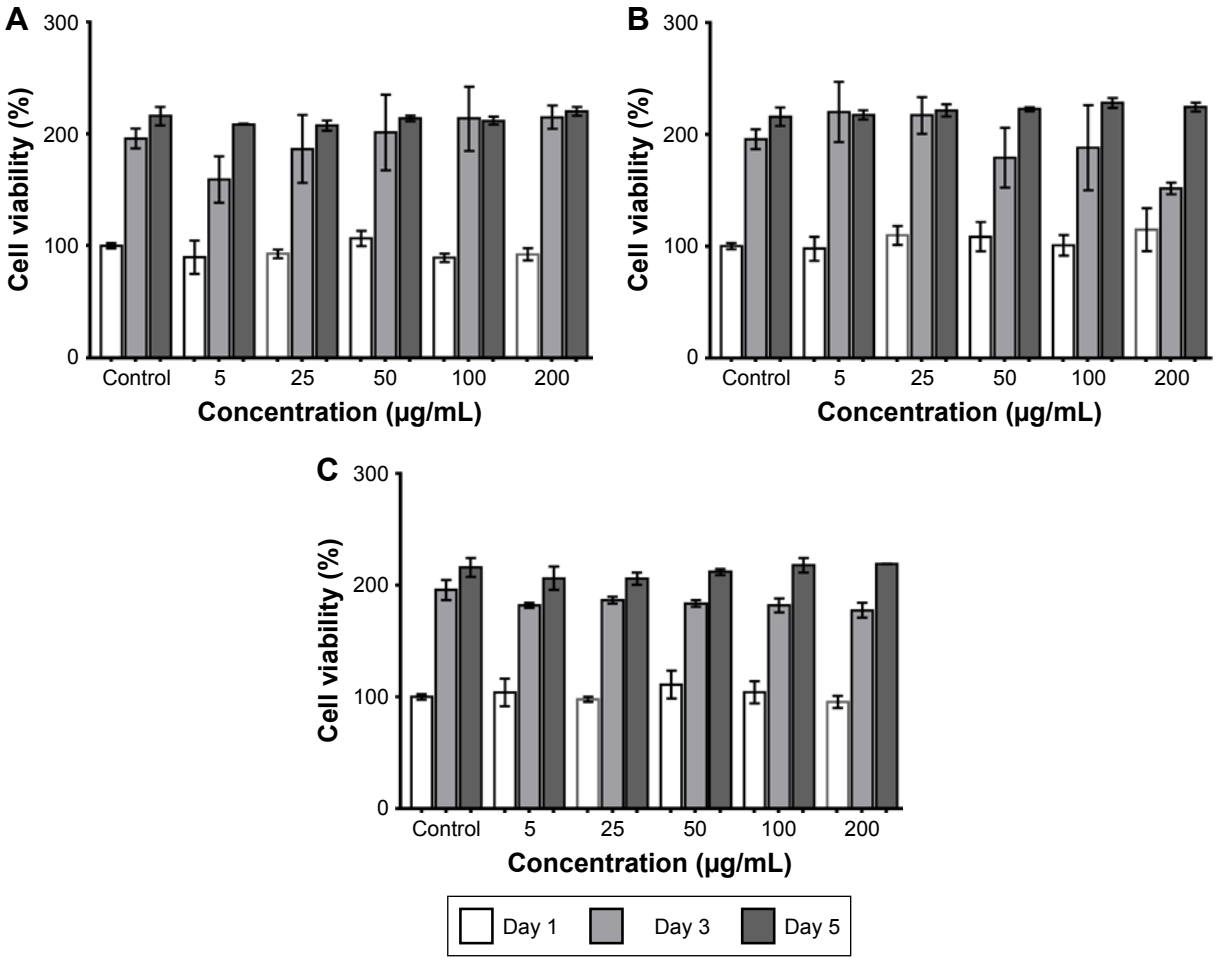

Figure S2 In vitro cytotoxicity of (**A**) FA-CPEG-AuNP, (**B**) FA-MAP-AuNP, and (**C**) FA-TAP-AuNP on HDFs.
Abbreviations: AuNP, gold nanoparticles; CPEG, citrate polyethylene glycol; FA, folate; HDFs, human dermal fibroblasts; MAP, malate polyethylene glycol; TAP, tartrate polyethylene glycol.

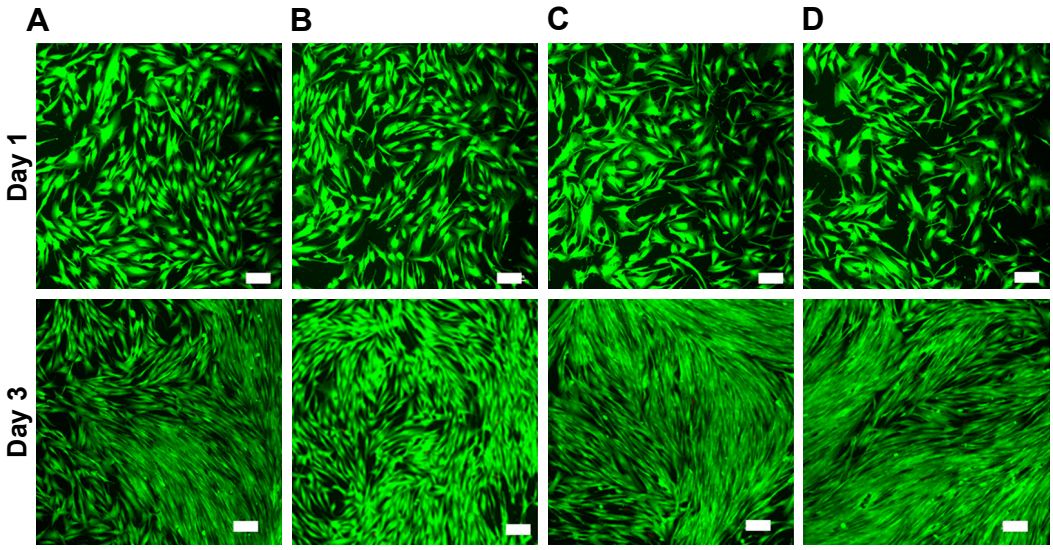

Figure S3 Live and dead fluorescence staining images of (**A**) control HDFs, (**B**) FA-CPEG-AuNPs, (**C**) FA-MAP-AuNPs, and (**D**) FA-TAP-AuNPs (at 100 μg/mL) treated HDFs after day 1 and 3 of incubation periods (scale bar=100 μm).

Abbreviations: AuNP, gold nanoparticles; CPEG, citrate polyethylene glycol; FA, folate; HDFs, human dermal fibroblasts; MAP, malate polyethylene glycol; TAP, tartrate polyethylene glycol.